

Detection of sequential polyubiquitylation on a millisecond timescale

Nathan W. Pierce¹, Gary Kleiger¹, Shu-ou Shan^{2*} & Raymond J. Deshaies^{1*}

The pathway by which ubiquitin chains are generated on substrate through a cascade of enzymes consisting of an E1, E2 and E3 remains unclear. Multiple distinct models involving chain assembly on E2 or substrate have been proposed. However, the speed and complexity of the reaction have precluded direct experimental tests to distinguish between potential pathways. Here we introduce new theoretical and experimental methodologies to address both limitations. A quantitative framework based on product distribution predicts that the really interesting new gene (RING) E3 enzymes SCF^{Cdc4} and SCF^{β-TrCP} work with the E2 Cdc34 to build polyubiquitin chains on substrates by sequential transfers of single ubiquitins. Measurements with millisecond time resolution directly demonstrate that substrate polyubiquitylation proceeds sequentially. Our results present an unprecedented glimpse into the mechanism of RING ubiquitin ligases and illuminate the quantitative parameters that underlie the rate and pattern of ubiquitin chain assembly.

Attachment of a polyubiquitin chain with at least four ubiquitins linked together through their lysine 48 residue (Lys 48) targets proteins to the proteasome for degradation¹. A cascade of three enzymes performs the synthesis of polyubiquitin chains: a ubiquitin-activating enzyme (E1), a ubiquitin-conjugating enzyme (E2) and a ubiquitin ligase (E3)². RING E3 enzymes catalyse the direct transfer of ubiquitin from an E2 to a lysine on a target protein³. SCF^{Cdc4} is the founding member of the largest family of E3 enzymes—the cullin-RING ubiquitin ligases that may comprise most of all human ubiquitin ligases³. Thus, unravelling the mechanism of SCF will have broad functional ramifications for the preponderance of human E3 enzymes.

Different pathways for ubiquitin chain assembly by RING E3 enzymes have been envisioned based on indirect evidence. On the one hand, Cdc34–SCF ubiquitylates substrates bearing a single ubiquitin significantly faster than non-ubiquitylated substrates^{4,5}, suggesting that it processively builds polyubiquitin chains on substrates with an initial slow transfer of ubiquitin followed by rapid elongation into a Lys-48-linked polyubiquitin chain. On the other hand, the E2 Ube2g2, a close relative of Cdc34, collaborates with the E3 gp78 to build a polyubiquitin chain on its active site cysteine that can be transferred en bloc to substrate^{6,7}. Various permutations of the en bloc mechanism have been entertained, in which the chain is built either from proximal to distal end or vice versa^{8–10}. Owing to the rapid speed of ubiquitin chain synthesis, intermediates that would reveal the underlying pathway cannot be kinetically resolved. Thus, it has not been possible to establish definitively the pathway of chain assembly for any RING E3. Here we introduce new theoretical and experimental methodologies to address both limitations.

Quantitative analysis of product distribution

Processivity emerges from the relationships between reaction and dissociation rates for different product intermediates¹¹. To quantify the processivity of SCF, we established an assay capable of simultaneously monitoring the concentrations of substrate and its different ubiquitylated product intermediates. Our assay consisted of an engineered phosphopeptide substrate (CYCE) derived from human cyclin E1 (also

known as CCNE1) and purified *Saccharomyces cerevisiae* Cdc34–SCF^{Cdc4} (refs 5, 12). CYCE was selected because it is a defined, chemically homogeneous substrate that binds with high affinity to the substrate-binding pocket of SCF^{Cdc4} (refs 12, 13). Moreover, intact cyclin E is a substrate of SCF^{Cdc4} *in vivo*¹⁴ and the degron from CYCE can support turnover *in vivo* of an engineered substrate, Sic1, from which the endogenous degrons have been eliminated¹². To examine the simplest system that recapitulated the processive behaviour of Cdc34–SCF^{Cdc4}, we focused on single turnover reaction conditions containing an excess of SCF^{Cdc4} over radiolabelled CYCE. We initiated reactions by combining two pre-incubated mixtures: the ‘charged E2’ mixture containing ubiquitin, E1, ATP and Cdc34 was pre-incubated for 2 minutes to ensure the formation of saturating concentrations of Cdc34–ubiquitin thioesters (E2–Ub); and the ‘substrate–ligase’ mixture containing SCF and radiolabelled substrate was pre-incubated to ensure the formation of an enzyme–substrate complex. To maximize resolution of ubiquitin conjugates, the reaction products were fractionated on long SDS-polyacrylamide gels. Consistent with previous assays performed with Sic1 (ref. 5), conjugation of the Nedd8 homologue Rub1 to the Cdc53 subunit of budding yeast SCF^{Cdc4} did not alter the ubiquitylation kinetics of CYCE (Supplementary Fig. 1); thus all subsequent SCF^{Cdc4} assays were performed with unmodified E3.

Under these reaction conditions, CYCE was extensively polyubiquitylated by Cdc34–SCF^{Cdc4} within 30 s (reaction 1, Fig. 1a), and products containing at least six ubiquitins were visible within 10 s (Supplementary Fig. 1). Thus, with the time resolution offered by manual mixing, it was not apparent whether ubiquitin conjugates were formed by multiple sequential transfers of monoubiquitin or by en bloc transfer of pre-formed chains. However, we reasoned that quantitative analysis of the length distribution of polyubiquitin chains attached to CYCE during a single encounter with SCF might provide clues to the pathway of chain assembly. To determine the length distribution, we performed reactions with 1,000-fold excess chase of the unlabelled substrate peptide added to the ‘charged E2’ mixture (reaction 2, Fig. 1a). Under these conditions, radiolabelled substrate pre-bound to SCF was rapidly ubiquitylated, but upon dissociation

¹Howard Hughes Medical Institute, Division of Biology, MC 156-29, ²Division of Chemistry and Chemical Engineering, MC 147-75, California Institute of Technology, 1200 East California Boulevard, Pasadena, California 91125, USA.

*These authors contributed equally to this work.

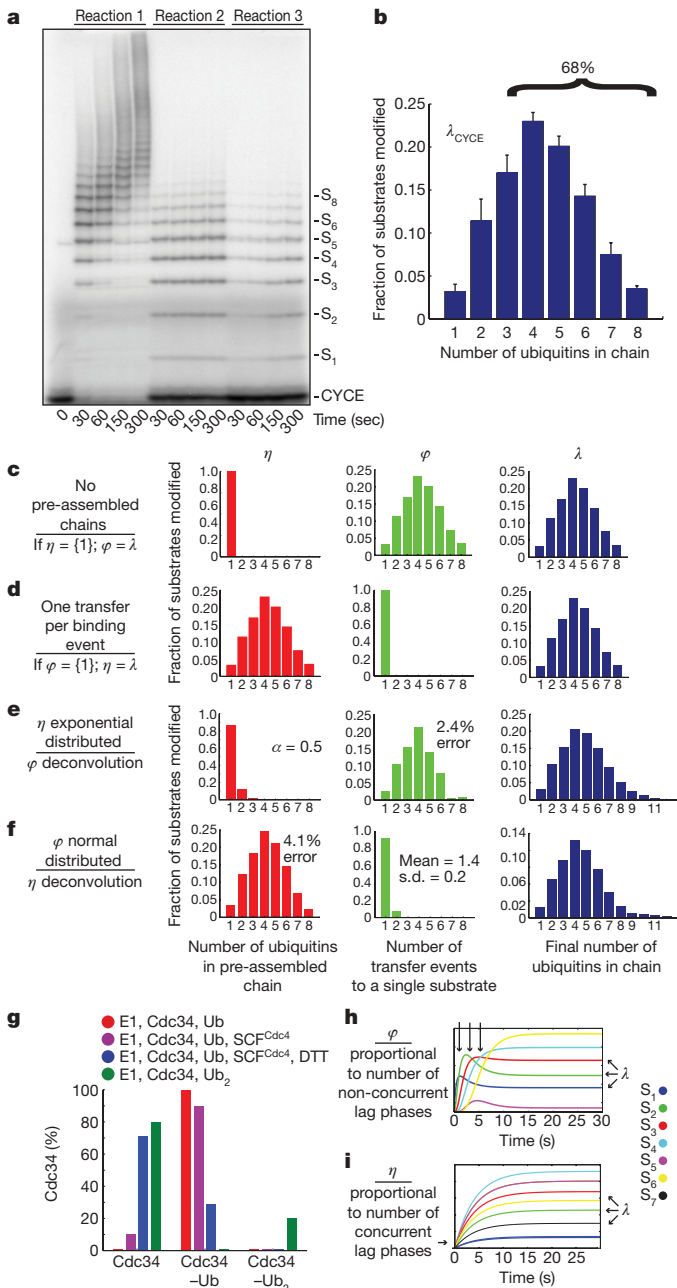


Figure 1 Final product distribution for SCF^{Cdc4} and CYCE. **a**, In reaction 1, pre-incubated ³²P-labelled CYCE and SCF^{Cdc4} were added to the charged E2 mix. In reactions 2 and 3, excess unlabelled CYCE was pre-incubated with charged E2 mix and labelled CYCE, respectively. **b**, The single-encounter polyubiquitin chain-length distribution, λ_{CYCE} . Error bars, \pm s.d. ($n = 3$). **c**, If $\eta(1) = 100\%$, then $\varphi = \lambda$. **d**, If $\varphi(1) = 100\%$, then $\eta = \lambda$. **e**, Deconvolution of λ_{CYCE} and exponentially distributed η . **f**, Deconvolution of λ_{CYCE} and normal distributed φ . **g**, Mass spectrometry of Cdc34 thioesterified for 2 min with indicated components. **h**, Simulated kinetics $\eta(1) = 100\%$. **i**, Simulated kinetics $\varphi(1) = 100\%$.

further ubiquitylation occurred at a significantly reduced rate due to competition from the chase peptide. To evaluate the effectiveness of the chase, we performed a parallel reaction in which the chase peptide was added to the 'substrate-ligase' mixture before initiation (reaction 3, Fig. 1a). The distribution of products in reaction 3 was subtracted from the distribution of products in reaction 2 at each time point (Supplementary Fig. 2) to yield the average distribution for substrate, λ (Fig. 1b). Three main points were highlighted by these experiments. First, it is evident from reaction 2 that the single-encounter reaction was complete within 30 s. Second, 72% of CYCE encounters with SCF^{Cdc4} resulted in no ubiquitin modification (Fig. 1a and

Supplementary Fig. 2). Third, of those substrates that were modified, 68% of CYCE acquired a polyubiquitin chain with four or more ubiquitins (Fig. 1b).

We next sought to develop a quantitative framework to address whether the experimentally determined product distribution λ_{CYCE} (Fig. 1b) places constraints on the potential pathways of ubiquitin chain assembly. We considered three hypothetical situations. First, we imagined that only monoubiquitin was attached in each transfer event (Fig. 1c, 'sequential'). Binning all of the transfer events per substrate gave the transfer distribution φ , which in this case would equal λ . Second, we imagined the other extreme in which only one transfer event occurs per substrate (Fig. 1d, 'en bloc'). In this case, λ would be equal to the distribution of pre-assembled polyubiquitin chains thioesterified to E2, which we named η . Third, we considered permutations that combined sequential and en bloc transfers. For example, there are eight possible ways of making substrate modified with four ubiquitins (S_n , where $n = 4$), including two transfers of diubiquitin or transfer of monoubiquitin followed by transfer of triubiquitin, etc. From this analysis, a key point emerged: regardless of the type of distribution we started with, the family of η and φ distributions compatible with λ_{CYCE} (see Supplementary Methods) was restricted to extreme cases where either η or φ was nearly equal to λ_{CYCE} (Fig. 1e, f and Supplementary Figs 3–7). Therefore, most substrates either underwent one transfer per binding event or received a single ubiquitin per transfer event. Thus, accurately measuring product distribution constrained the number of possible pathways that could give rise to the reaction products we observed.

As a first test of whether ubiquitins were transferred all at once or sequentially, we measured the distribution of polyubiquitin chain lengths present on the active site of Cdc34 in the presence or absence of SCF^{Cdc4} by intact mass spectrometry. Cdc34 subjected to our standard 'charged E2' pre-incubation was completely converted to thioesters carrying a single ubiquitin (Cdc34-Ub; Fig. 1g and Supplementary Fig. 10). In the presence of SCF^{Cdc4}, 89% of Cdc34 was detected as Cdc34-Ub and 11% was unmodified; no Cdc34 species with more than one ubiquitin attached was detected. A control experiment run with diubiquitin confirmed that our assay was able to detect diubiquitin chains thioesterified to the active site of Cdc34 (Cdc34-Ub₂; Supplementary Fig. 11), but charging of Cdc34 with diubiquitin occurs with poor efficiency ($\sim 20\%$). Thus, our analysis of the product distribution λ coupled with measurement of the ubiquitin population thioesterified to Cdc34 under our reaction conditions (an estimate of η) strongly predicts that Cdc34-SCF^{Cdc4} assembled ubiquitin chains on substrate primarily by sequential transfers of single ubiquitin molecules.

Millisecond kinetics of SCF

As a second, more definitive test of the hypothesis stated above, we sought to measure directly how the product distribution (Fig. 1b) developed as a function of time. During a single encounter between a RING ubiquitin ligase and substrate, each intermediate should either undergo a transfer event or dissociate. If monoubiquitin composed 100% of η as in Fig. 1c, the products of the reaction should appear sequentially in time starting with S_1 and followed by S_2 , then S_3 , etc. Thus, the appearance of each sequential product should be delayed by a 'lag' phase (Fig. 1h). In contrast, if a single transfer composed 100% of φ as in Fig. 1d, then the pattern of ubiquitin chains attached to substrate at the earliest time-points should reveal the distribution of pre-assembled chains thioesterified to Cdc34 (Fig. 1i). Thus, products of increasing mass should accumulate sequentially if chain synthesis is sequential, but should accumulate contemporaneously if chains are transferred en bloc. Therefore, with sufficient time resolution, a single-encounter experiment would provide definitive data to distinguish between the alternative models. To achieve the necessary time resolution, we performed our single-encounter reactions on a quench flow apparatus that allowed us to take measurements on a timescale ranging from 10 ms to 30 s (Fig. 2a). To facilitate quantification of S_2

and S_5 in the CYCE reaction, the same reaction from Fig. 2a was fractionated on a gel with different resolving capabilities (Supplementary Fig. 12). Three major conclusions arose from these experiments. First, the product CYCE-Ub (S_1) was formed starting at the earliest time points (10–20 ms) without a lag phase, indicating that E2-Ub binding to SCF was rapid. This is consistent with stopped-flow measurements performed with SCF ^{β -TrCP} and hCdc34 (ref. 15). Second, each new ubiquitylated product appeared sequentially with non-concurrent lag phases (Fig. 2a, b and Supplementary Fig. 12). Third, the early reaction products S_1 – S_3 ‘overshot’ their final levels, indicating that these reaction intermediates serve as templates for the formation of subsequent products, supporting the model that polyubiquitin chains are built from multiple transfer events (Supplementary Fig. 16). Combined with the constraints on η and φ calculated above as well as our direct evaluation of the Cdc34-Ub pool (Fig. 1g), these data demonstrate that the underlying kinetic mechanism of our system was principally derived from sequential transfers of single ubiquitins.

To ensure that our conclusions were not an artefact of the reaction design, we changed the order of addition in our reactions. SCF^{Cdc4} was pre-incubated with the ‘charged E2’ mixture for 2 min (in which case 89% of Cdc34 is present in thioesterified form; Fig. 1g) and reactions were initiated by combining with radiolabelled CYCE. Products appeared after non-concurrent lag phases of increasing duration (Fig. 2c), analogous to that observed when the reaction was initiated by addition of Cdc34-Ub to CYCE prebound to SCF^{Cdc4} (Fig. 2a). Thus, regardless of whether CYCE first encountered Cdc34-Ub-SCF or Cdc34-Ub encountered CYCE-SCF, single ubiquitins were transferred to substrate in a sequential manner. Interestingly, reactions initiated by addition of CYCE were delayed compared with those initiated by addition of Cdc34-Ub, indicating that Cdc34-Ub productively associates with SCF^{Cdc4} faster than does CYCE.

SCF ^{β -TrCP} is sequentially processive

We next sought to test whether the sequential processive chain assembly we observed for SCF^{Cdc4} is unique or illuminates a general

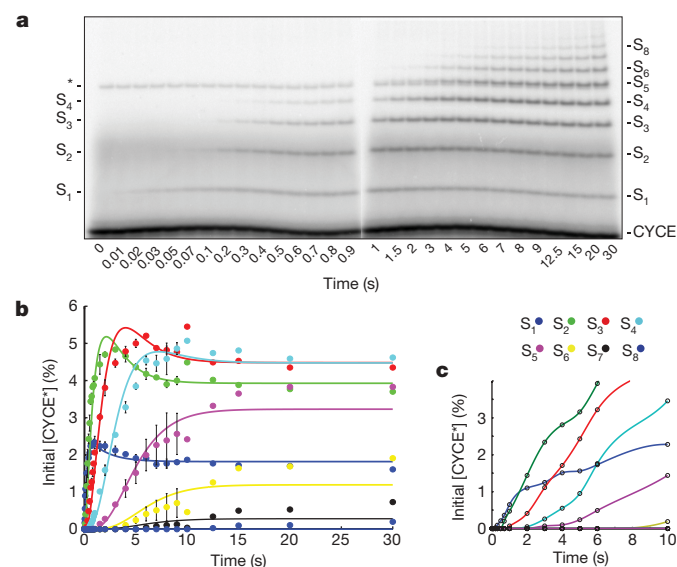


Figure 2 | Millisecond kinetics of a single-encounter reaction reveal sequential processivity. **a**, To achieve millisecond temporal resolution, CYCE reactions were performed on a quench flow apparatus and products were evaluated by SDS–polyacrylamide gel electrophoresis and phosphorimaging. The reaction scheme matched reaction 2 of Fig. 1a. The asterisk marks a contaminant. S_n refers to CYCE modified with n ubiquitins. **b**, Quantification shows successively longer lag phases for each additional ubiquitin added in the chain. The data were fitted using closed-form solutions refined by global regression analysis to a model with $\eta = 1$. The error bars represent the range of values ($n = 2$). **c**, SCF^{Cdc4} was pre-incubated with charged E2 mix and combined with ³²P-labelled CYCE.

principle of SCF ubiquitin ligase mechanism. To address this issue, we evaluated ubiquitylation of a phosphopeptide derived from β -catenin (β -Cat) by its cognate E2–E3 complex, hCdc34 and human SCF ^{β -TrCP}. Nedd8-conjugated E3 (N8-SCF ^{β -TrCP}) was used for these experiments, because previous work demonstrated a potent stimulation of β -Cat ubiquitylation upon Nedd8 conjugation⁴. As was seen with CYCE–SCF^{Cdc4}, β -Cat was rapidly modified by N8-SCF ^{β -TrCP} and it was not possible to resolve intermediates in chain assembly by manual mixing⁴ (Fig. 3a). Quantification of product distribution $\lambda_{\beta\text{-Cat}}$ revealed that 6% of β -Cat molecules were modified in a single encounter with N8-SCF ^{β -TrCP}, of which 85% received at least four ubiquitins (Fig. 3b and Supplementary Fig. 2). Distribution analysis of $\lambda_{\beta\text{-Cat}}$ (Fig. 3c) and kinetic resolution of β -Cat ubiquitylation by quench-flow (Fig. 3d, e) revealed sequential appearance of intermediates analogous to those observed with CYCE ubiquitylation by SCF^{Cdc4}.

Although the general behaviour of SCF^{Cdc4} and N8-SCF ^{β -TrCP} were similar, the enzymes differed in the extent to which they

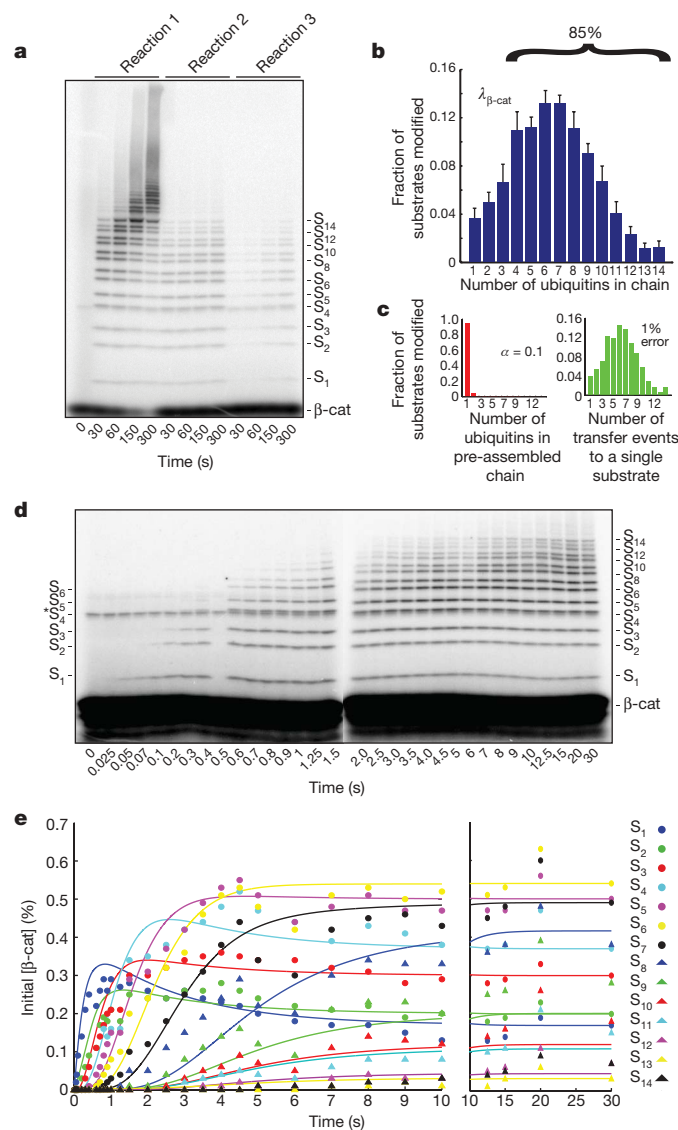


Figure 3 | Human Cdc34–SCF ^{β -TrCP} is sequentially processive. **a**, The same as Fig. 1a, except that human Cdc34 and Nedd8-conjugated SCF ^{β -TrCP} were assayed with ³²P-labelled β -Cat substrate. **b**, Product distribution ($\lambda_{\beta\text{-Cat}}$) was quantified as in Fig. 1b. Error bars, \pm s.d. ($n = 3$). **c**, The Poisson distribution of φ using $\lambda_{\beta\text{-Cat}}$ that deviated the most from $\varphi(1) = 100\%$ within our set error bounds with $\alpha = 0.2$. **d**, β -Cat reactions with the scheme of reaction 2 (Fig. 1a) performed on a quench flow apparatus. **e**, Quantification shows successively lengthening lag phases for each additional ubiquitin added in the chain. The data were fitted as in Fig. 2b.

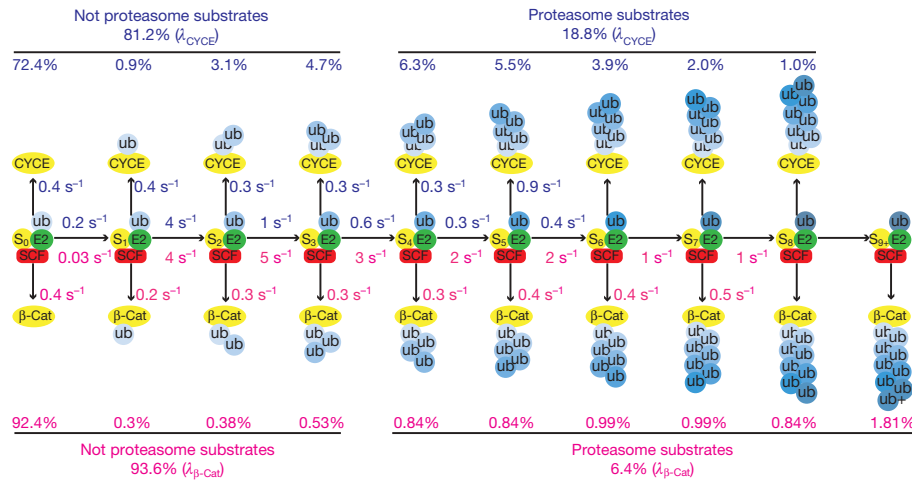


Figure 4 | Kinetic basis for Cdc34–SCF processivity. The millisecond kinetics of a single-encounter reaction were fitted to a sequential model revealing estimates for individual transfer and dissociation rates for each intermediate in

converted bound substrate to product and elongated ubiquitin chains. Using a kinetic model in which monoubiquitin composed 100% of η , we were able to use methods borrowed from the study of nucleic acid polymerases¹⁶ to extrapolate estimates for the individual reaction and dissociation rate constants from our single-encounter quench-flow experiments (Fig. 4 and Supplementary Figs 13–15).

Functional implications of our model

The model shown in Fig. 4 reveals the kinetic basis of processive polyubiquitin chain synthesis by budding yeast Cdc34–SCF^{Cdc4} and human Cdc34–SCF ^{β -TrCP}, and accounts for the differences in their behaviour. Most encounters of substrate and SCF are unproductive because k_{off} is faster than k_{Ub1} . This is particularly exaggerated for β -Cat owing to its low value for k_{Ub1} . Once a single ubiquitin is attached, most substrates are committed to polyubiquitylation because of the drastic increase in k_{Ub2} relative to a nearly constant k_{off} . This gives rise to the high percentage of modified substrates with four or more ubiquitins in their chain (68% for CYCE and 85% for β -Cat). The overall chain length is limited by the progressive decrease in transfer rates ($k_{\text{Ub}n}$) as the chain becomes longer matched against the relatively constant rate at which product intermediates dissociate. This reduction in transfer rate most likely arises because the distal end of the flexible chain samples a progressively larger volume as it increases in length¹⁷. The longer chains on β -Cat are a result of a less dramatic decline in $k_{\text{Ub}n}$ after the second ubiquitin is attached. We do not understand the basis for this difference. Meanwhile, the constant rate of dissociation for both CYCE and β -Cat implies that ubiquitin chains of increasing length do not change the intrinsic affinity of these substrates for SCF.

Casual inspection of our model suggests that modest changes in the ratio $k_{\text{Ub1}}/k_{\text{off}}$ for the first step would substantially alter the fraction of substrate that acquires a chain of at least four ubiquitins in a single encounter with SCF. This in turn provides a simple basis for SCF to modulate a substrate's degradation half-life (that is, the larger k_{off} is or smaller k_{Ub1} is, the lower the probability that a substrate is modified in a single encounter with SCF, which would translate to a longer half-life). Comparison of CYCE and β -Cat, which have distinct $k_{\text{Ub1}}/k_{\text{off}}$ ratios, underscores how the efficiency and pattern of substrate ubiquitylation can be tuned by these parameters. Despite these differences, it is remarkable how similar the reaction parameters are for two different enzymes from organisms separated by over 1 billion years of evolution. In both cases, k_{off} was about 0.4 s^{-1} and the fastest rate of ubiquitin chain elongation was $4\text{--}5 \text{ s}^{-1}$. This suggests that true substrates are tuned to dissociate within a few seconds and that a transfer rate of 5 s^{-1} may be imposed by a conserved rate-limiting step. It will be of great interest to determine what molecular event enforces this speed limit.

the generation of polyubiquitinated CYCE (blue numbers) and β -Cat (red numbers) products. The percentages listed above or below each product were those from the final product distributions (λ) shown in Figs 1b and 3b.

We conclude that polyubiquitin chains are built on SCF substrates by sequential transfers of single ubiquitins. We establish a mechanistic framework that can be applied to other cullin–RING ubiquitin ligases and RING ubiquitin ligases to obtain individual rate constants for substrate dissociation and ubiquitin transfer at each step in the process of chain assembly. Our model indicates that the processivity, efficiency and pattern of ubiquitylation is governed by the sharp discontinuity in rates between the first transfer and subsequent transfers, contrasted with the shared dissociation rate among substrate and product intermediates.

METHODS SUMMARY

Proteins. CYCE and β -Cat phosphopeptide were purchased from New England Peptide. Ubiquitin and K48 diubiquitin were purchased from Boston Biochem. Uba1 and SCF^{Cdc4} were prepared and purified as described⁷. Full-length yeast Cdc34 was purified as described¹⁸. His7–Rub1 was purified from *Escherichia coli* inclusion bodies⁴ and human E1, UbcH3B (hCdc34) and Nedd8–SCF ^{β -TrCP} were prepared and purified as described⁴. Yeast Ubc12 and Ula1–Uba3 were purified as described¹⁹. Rub1, Ubc12, Ula1–Uba3 and ATP were incubated with immobilized SCF^{Cdc4} to make Rub1-conjugated SCF^{Cdc4}. Protein kinase A was purchased from New England Biolabs.

Ubiquitylation assay. CYCE (200 nM) or β -Cat (2 μM) was incubated with [γ -³²P]ATP (132 nM) and protein kinase A for 45 min at 30 °C to make radiolabelled CYCE or β -Cat. Yeast ubiquitylation reactions contained ATP (2 mM), ubiquitin (60 μM), Uba1 (0.8 μM), Cdc34 (10 μM), SCF^{Cdc4} (150 nM) and radiolabelled CYCE (10 nM).

Human ubiquitylation reactions contained ATP (2 mM), ubiquitin (60 μM), E1 (1 μM), Cdc34 (10 μM), SCF ^{β -TrCP} (500 nM) and radiolabelled β -Cat (100 nM). As indicated, single-encounter reactions contained an unlabelled CYCE chase (10 μM) or β -Cat chase (100 μM). Millisecond reactions were performed on a quench flow apparatus (Kintek RQF-3 Rapid Quench Flow). Reactions contained a buffer previously described²⁰ at 23 °C. Reactions were quenched with SDS–polyacrylamide gel electrophoresis buffer with β -mercaptoethanol and run on 20-cm 5–20% tricine gels (CYCE) or glycine gels (β -Cat) that were quantified with a phosphor screen (Molecular Devices). Thioester formation assays contained Cdc34 (10 μM), Uba1 (1 μM), ATP (2 mM), ubiquitin or K48 diubiquitin (15 μM) and SCF^{Cdc4} (100 nM) as indicated. After 2 min, reactions were stopped with excess 5% acetic acid and analysed on an Agilent LC-MSD.

Analysis. Deconvolutions and regression were performed in Matlab. Global fitting was performed with KinTek Global Kinetic Explorer. Mass spectrometry data were processed using the Chemstation software package.

Full Methods and any associated references are available in the online version of the paper at www.nature.com/nature.

Received 25 September; accepted 19 October 2009.

1. Thrower, J. S. *et al.* Recognition of the polyubiquitin proteolytic signal. *EMBO J.* 19, 94–102 (2000).

2. Dye, B. T. & Schulman, B. Structural mechanisms underlying posttranslational modification by ubiquitin-like proteins. *Annu. Rev. Biophys. Biomol. Struct.* **36**, 131–150 (2007).
3. Petroski, M. & Deshaies, R. Function and regulation of cullin–RING ubiquitin ligases. *Nature Rev. Mol. Cell Biol.* **6**, 9–20 (2005).
4. Saha, A. & Deshaies, R. Multimodal activation of the ubiquitin ligase SCF by Nedd8 conjugation. *Mol. Cell* **32**, 21–31 (2008).
5. Petroski, M. & Deshaies, R. Mechanism of lysine 48-linked ubiquitin-chain synthesis by the cullin–RING ubiquitin-ligase complex SCF–Cdc34. *Cell* **123**, 1107–1120 (2005).
6. Ravid, T. & Hochstrasser, M. Autoregulation of an E2 enzyme by ubiquitin-chain assembly on its catalytic residue. *Nature Cell Biol.* **9**, 422–427 (2007).
7. Li, W. *et al.* A ubiquitin ligase transfers preformed polyubiquitin chains from a conjugating enzyme to a substrate. *Nature* **446**, 333–337 (2007).
8. Hochstrasser, M. Lingering mysteries of ubiquitin-chain assembly. *Cell* **124**, 27–34 (2006).
9. Li, W. *et al.* Mechanistic insights into active site-associated polyubiquitination by the ubiquitin-conjugating enzyme Ube2g2. *Proc. Natl Acad. Sci. USA* **106**, 3722–3727 (2009).
10. Deshaies, R. J. & Joazeiro, C. A. RING domain E3 ubiquitin ligases. *Annu. Rev. Biochem.* **78**, 399–434 (2009).
11. Fersht, A. *Structure and Mechanism in Protein Science: A Guide to Enzyme Catalysis and Protein Folding* Ch. 14 (Freeman, 1999).
12. Nash, P. *et al.* Multisite phosphorylation of a CDK inhibitor sets a threshold for the onset of DNA replication. *Nature* **414**, 514–521 (2001).
13. Orlicky, S. *et al.* Structural basis for phosphodependent substrate selection and orientation by the SCF^{Cdc4} ubiquitin ligase. *Cell* **112**, 243–256 (2003).
14. Strohmaier, H. *et al.* Human F-box protein hCdc4 targets cyclin E for proteolysis and is mutated in a breast cancer cell line. *Nature* **413**, 316–322 (2001).
15. Kleiger, G., Saha, A., Lewis, S., Kuhlman, B. & Deshaies, R. Rapid E2–E3 assembly and disassembly enable processive ubiquitylation of cullin–RING ubiquitin ligase substrates. *Cell*. (in the press).
16. Kati, W. M. *et al.* Mechanism and fidelity of HIV reverse transcriptase. *J. Biol. Chem.* **267**, 25988–25997 (1992).
17. Petroski, M. *et al.* Evaluation of a diffusion-driven mechanism for substrate ubiquitination by the SCF–Cdc34 ubiquitin ligase complex. *Mol. Cell* **24**, 523–534 (2006).
18. Feldman, R. M. *et al.* A complex of Cdc4p, Skp1p, and Cdc53p/cullin catalyzes ubiquitination of the phosphorylated CDK inhibitor Sic1p. *Cell* **91**, 221–230 (1997).
19. Kamura, T. *et al.* The Rbx1 subunit of SCF and VHL E3 ubiquitin ligase activates Rub1 modification of cullins Cdc53 and Cul2. *Genes Dev.* **13**, 2928–2933 (1999).
20. Petroski, M. & Deshaies, R. *In vitro* reconstitution of SCF substrate ubiquitination with purified proteins. *Methods Enzymol.* **398**, 143–158 (2005).

Supplementary Information is linked to the online version of the paper at www.nature.com/nature.

Acknowledgements We thank J. Vielmetter for providing SCF^{Cdc4}, β -TrCP–Skp1 and human E1; S. Hess, R. L. J. Graham and the Proteome Exploration Laboratory for providing assistance with mass spectrometry of CYCE and Cdc34 thioester. We thank S. Schwarz, B. Schulman and G. Wu for gifts of reagents. We thank D. Sprinzak and all the members of the Deshaies and Shan laboratories for support and discussions. N.W.P. was supported by the Gordon Ross Fellowship and a National Institutes of Health Training Grant. R.J.D. is an Investigator of the Howard Hughes Medical Institute. This work was supported in part by National Institutes of Health GM065997.

Author Contributions N.W.P. performed all computational modelling and experiments, except G.K. performed the mass spectrometry experiments in Fig. 1g. N.W.P., R.J.D. and S.-o.S. conceived the experiments. N.W.P. and R.J.D. wrote the manuscript with editorial input from the other authors.

Author Information Reprints and permissions information is available at www.nature.com/reprints. Correspondence and requests for materials should be addressed to R.J.D. (deshaies@caltech.edu).

METHODS

RDB 2289 with pGEX2-T His7-Rub1 was made by cloning a His7 tag in place of the GST tag in RDB 1436. To make Rub1-conjugated SCF^{Cdc4}, the procedure for isolating SCF^{Cdc4} was modified²⁰. Instead of eluting SCF^{Cdc4} from Py-conjugated protein A beads after washing, 50 μ M Rub1, 10 μ M Ubc12, 1 μ M Ula1-Uba3 and 2 mM ATP were incubated together overnight. The beads were washed before elution.

For all reactions, gels were dried and exposed to phosphor screens (Molecular Dynamics). Images were scanned and then quantified in ImageQuant using a rolling ball background subtraction. For each lane, every band was quantified as a percentage of the total signal in all bands.

The relation between η , φ and λ was mathematically analogous to the probability of the sum of multiple dice throws. However, the probability of throwing each number on the dice was a weighted normalized distribution (analogous to η) and the number of throws was also a weighted normalized distribution (analogous to φ). A distribution that is normalized sums to 1. Thus, λ equalled the weighted sum of multiple discrete convolutions of η with itself as governed by φ , as shown by example in Supplementary Fig. 3. Knowledge of λ and η allowed us to calculate φ by multiple weighted deconvolutions, as shown by example in Supplementary Fig. 4. This was true for calculating η from λ and φ , as shown by example in Supplementary Fig. 5a. If we assigned a distribution to η , we determined φ by deconvolutions with λ , and vice versa. Considering normalized distributions of η that only contained $\eta(1)$ and $\eta(2)$, exponential distributions, Poisson distributions and normal distributions, we varied parameters over a wide range and performed deconvolutions, as shown by example in Supplementary Fig. 5b. An exponential distribution is described by a single parameter, here called α . A Poisson distribution is also described by a single parameter, here called α . The normal distribution is described by two parameters, the mean and the standard deviation (s.d.). Parameters were varied starting at 0 and increasing by step sizes of 0.1 until they equalled 10. For the normal distribution, each value of the mean was held constant while the s.d. was varied. We sought the distribution that deviated most from $\eta(1) = 100\%$ whose φ did not contain values >1 or <0 and that when convoluted with φ , the sum of λ fell within 0.95 and 1.05, or an error rate of $\pm 5\%$ was found. This was repeated for φ . These distributions are shown in Supplementary Figs 6 and 7. Random distributions were also considered (data not shown).

For mass spectrometry analysis, Uba1 (1 μ M), Cdc34- Δ 270 (10 μ M) and ubiquitin or K48-linked di-ubiquitin (15 μ M, Boston Biochem) were incubated for

2 min in reaction buffer (30 mM Tris, pH 7.5, 100 mM NaCl, 5 mM MgCl₂, 2 mM dithiothreitol and 2 mM ATP) in a volume of 10 μ l both in the presence and absence of SCF (100 nM). Reactions were quenched by the addition of 90 μ l 5% acetic acid. Quenching was verified by an order of addition reaction where E1 was left out of the initial incubation and was added after quenching. This resulted in 100% quenching of the thioester charging reaction. Separation of E2 thioesters in the presence of SCF was accomplished by the addition of 100 mM dithiothreitol after the 2 min incubation period. The dithiothreitol was incubated with the reaction mixture for 5 min followed by the addition of 90 μ l of 5% acetic acid. Detection of proteins was done on an Agilent LC-MSD. Mass spectra were acquired in positive-ion mode, scanning from 500 to 1700 *m/z*. The electrospray voltage was set to 4 kV and the gas temperature in the spray chamber was maintained at 350 °C. A stationary phase, Zorbax 300SB C3 150 mm \times 2.1 mm column was used for separation (Agilent). Mobile phase A was 0.2% formic acid; mobile phase B was 0.2% formic acid, 10% methanol and 90% acetonitrile. The flow rate was 0.200 ml min⁻¹. After a 25-min delay, the effluent was directed into the mass spectrometer. Linear gradients started with 5% mobile phase B and finished at 95% from 25–50 min. Data were processed using the ChemStation software package. The sequence of yeast Cdc34- Δ 270 contains the amino acids from positions 1 to 270 of the yeast Cdc34 sequence followed by the sequence ARPLHHHHHH, yielding a theoretical molecular mass of 32,245 daltons. The theoretical mass of Cdc34- Δ 270 thioesterified with ubiquitin (40,792) was calculated by summing the masses of Cdc34- Δ 270 (32,245) and ubiquitin (8,565) and subtracting the mass of a water molecule, which is lost during formation of the thioester bond.

For CYCE global fitting with KinTek Global Kinetic Explorer, the average of two independent experiments was fitted to a model with $\eta = 1$, and the fit for k_1 – k_4 used the normalized option whereas the rest of the rate constants did not. For β -Cat global fitting, rate constants were fitted without normalization. To improve fitting, neighbouring rate constants were constrained by the end point. The dissociation constants (K_d) for CYCE/Cdc4 (ref. 21) and β -Cat/ β -TrCP²² were used to derive starting concentrations of bound substrate.

- Hao, B. *et al.* Structure of a Fbw7-Skp1-cyclin E complex: multisite-phosphorylated substrate recognition by SCF ubiquitin ligases. *Mol. Cell* **26**, 131–143 (2007).
- Wu, G. *et al.* Structure of a β -TrCP1-Skp1- β -catenin complex. *Mol. Cell* **11**, 1445–1456 (2003).